

1 *Chem. Pharm. Bull.*

2 *Regular Article*

3 **Enhancing the Solubility and Oral Bioavailability of Poorly Water-Soluble**  
4 **Drugs using Monoolein Cubosomes**

5 Md. Ashraf Ali,<sup>a,b</sup> Noriko Kataoka,<sup>a</sup> Abdul-Hackam Ranneh,<sup>a</sup> Yasunori Iwao,<sup>a</sup> Shuji  
6 Noguchi,<sup>a</sup> Toshihiko Oka,<sup>c</sup> and Shigeru Itai\*<sup>a</sup>

7  
8 *<sup>a</sup>Department of Pharmaceutical Engineering & Drug Delivery Science, Graduate School of*  
9 *Integrated Pharmaceutical & Nutritional Sciences, University of Shizuoka; 52-1 Yada,*  
10 *Suruga-ku, Shizuoka 422-8526, Japan.*

11 *<sup>b</sup>Department of Pharmacy, Faculty of Life Science, Mawlana Bhashani Science and*  
12 *Technology University, Santosh, Tangail-1902, Bangladesh*

13 *<sup>c</sup>Department of Physics, Faculty of Science and Nanomaterials Research Division, Research*  
14 *Institute of Electronics, Shizuoka University; 836 Oya, Suruga-ku, Shizuoka 422-8529, Japan.*

15  
16 \*Address correspondence to:

17 Shigeru Itai, Ph.D.

18 Professor

19 Department of Pharmaceutical Engineering & Drug Delivery Science

20 Graduate School of Integrated Pharmaceutical & Nutritional Sciences

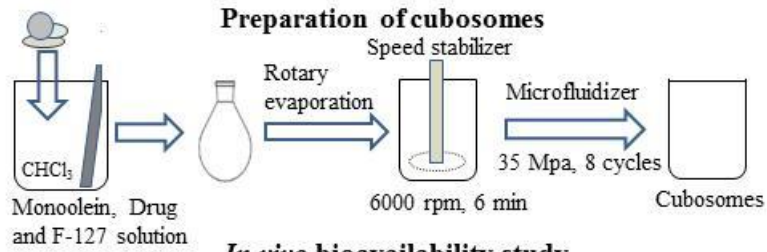
21 University of Shizuoka

22 52-1 Yada, Suruga-ku, Shizuoka 422-8526, Japan

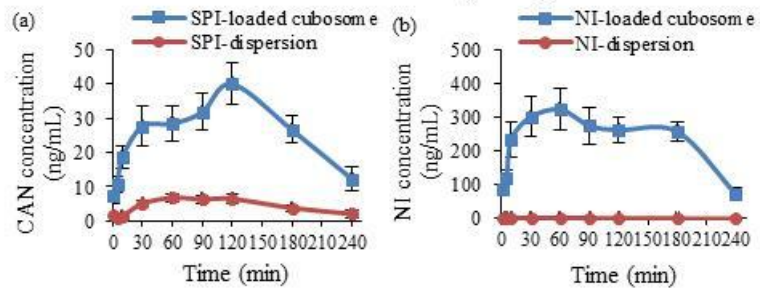
23 Tel.: +81 54 264 5614, Fax: +81 54 264 5615.

24 E-mail: s-itai@u-shizuoka-ken.ac.jp

# Graphical abstract



## *In vivo* bioavailability study



25

26

27

28

29

30

31

32

33

34

35

36

37

38

39

## 40 **Summary**

41 Monoolein cubosomes containing either spironolactone (SPI) or nifedipine (NI) were  
42 prepared using a high-pressure homogenization technique and characterized in terms of their  
43 solubility and oral bioavailability. The mean particle size, polydispersity index (PDI), zeta  
44 potential, solubility and encapsulation efficiency (EE) values of the SPI- and NI-loaded  
45 cubosomes were determined to be 90.4 nm, 0.187, -13.4 mV, 163  $\mu\text{g/mL}$  and 90.2%, and  
46 91.3 nm, 0.168, -12.8 mV, 189  $\mu\text{g/mL}$  and 93.0%, respectively, which were almost identical  
47 to those of the blank cubosome. Small-angle X-ray scattering analyses confirmed that the  
48 SPI-loaded, NI-loaded and blank cubosomes existed in the cubic space group  $Im\bar{3}m$ . The  
49 lattice parameters of the SPI- and NI-loaded cubosomes were 147.6 and 151.6  $\text{\AA}$ , respectively,  
50 making them almost identical to that of blank cubosome (151.0  $\text{\AA}$ ). The *in vitro* release  
51 profiles of the SPI- and NI-loaded cubosomes showed that they released less than 5% of the  
52 drugs into various media over 12–48 h, indicating that most of the drug remained  
53 encapsulated within the cubic phase of their lipid bilayer. Furthermore, the *in vivo*  
54 pharmacokinetic results suggested that these cubosomes led to a considerable increase in the  
55 systemic oral bioavailability of the drugs compared with pure dispersions of the same  
56 materials. Notably, the stability results indicated that the mean particle size and PDI values of  
57 these cubosomes were stable for at least 4 weeks. Taken together, these results demonstrate  
58 that monoolein cubosomes represent promising drug carriers for enhancing the solubility and  
59 oral bioavailability of poorly water-soluble drugs.

60

61 **Keywords:** cubosome; drug carrier; monoolein; nifedipine; spironolactone; high-pressure  
62 homogenization.

63

64

## 65 **Introduction**

66 The low oral bioavailability of poorly water-soluble drugs remains one of the most  
67 challenging aspects of drug development. A wide variety of formulation approaches,  
68 including lipid nanoparticles, solid dispersions, complexes with cyclodextrin or chitosan-  
69 alginates, nanoemulsions and liposomes, have been used to enhance the solubility and  
70 bioavailability of several poorly water-soluble drugs.<sup>1-5)</sup> Cubosomes have recently attracted  
71 considerable interest from formulation scientists in terms of their potential application as drug  
72 delivery systems based on their highly ordered, compartmentalized internal structures, high  
73 lipid content and large surface area.

74 Cubosomes are inverse bicontinuous cubic lyotropic crystalline nanoparticles that can be  
75 loaded with poorly water-soluble drugs in their three-dimensional cubic phases, leading to  
76 pronounced increases in the solubility, stability and bioavailability of these drugs.<sup>6-9)</sup>  
77 Cubosomes can be prepared using nontoxic, biocompatible and biodegradable ingredients,  
78 and can be readily used to encapsulate lipophilic drugs. Monoolein is a common amphiphilic  
79 building block for the preparation of cubosomes,<sup>10)</sup> and is relatively cheap compared with  
80 other commonly used lipid excipients such as phytantriol. Nonionic triblock copolymer  
81 (Pluronic F-127) is an excellent steric stabilizer that can be used to stabilize the structures of  
82 cubosomes and prevent particle aggregation for extended periods of time.<sup>11)</sup> Monoolein cubic  
83 nanoparticles and cubosomes have recently been proposed as potential drug carriers because  
84 they can (i) efficiently encapsulate poorly water-soluble drugs and enhance their solubility;  
85 (ii) exhibit bio-adhesive properties with sustained release properties; (iii) protect drug  
86 molecules and increase their duration of action; and (iv) improve the oral bioavailability of  
87 poorly water-soluble drugs.<sup>9, 12-14)</sup> The results of several studies have shown that the  
88 encapsulation of 20(S)-protopanaxadiol, simvastatin and amphotericin B in monoolein  
89 cubosomes and/or cubic nanoparticles led to increases in the oral bioavailabilities of these

90 poorly water-soluble drugs.<sup>15-17)</sup> However, there have been very few studies in the literature  
91 pertaining to the *in vivo* evaluation of cubosomes. Given that lipid-based formulations have  
92 been used in drug delivery to improve the oral absorption of poorly water-soluble drugs for  
93 many years,<sup>18-20)</sup> we envisaged that cubosomes could also increase their bioavailability.

94 In this study, we used spironolactone (SPI) and nifedipine (NI) as model drugs to prepare  
95 SPI- and NI-loaded cubosomes using a high-pressure homogenization technique. The drug  
96 loaded cubosomes were subsequently evaluated in terms of their particle size distribution,  
97 particle stability, solubility, and encapsulation efficiency characteristics. We also evaluated  
98 the *in vitro* release rate and oral bioavailability properties of the cubosomes for the  
99 encapsulated drugs.

100

## 101 **Experimental**

### 102 **Materials**

103 Monoolein (-OL-100H) was provided as a gift from Riken Vitamin Co., Ltd (Tokyo,  
104 Japan). Pluronic F-127 was gifted from BASF (Ludwigshafen, Germany). Spironolactone and  
105 nifedipine were purchased from Tokyo Chemical Co., Ltd (Tokyo, Japan) and Sagami Kasei  
106 (Tokyo, Japan), respectively. Chloroform, methanol and formic acid were purchased from  
107 Wako Chemical Industries, Ltd (Osaka, Japan). All of the other reagents used in this study  
108 were purchased as the highest grades available from commercial sources.

### 109 **Preparation of Cubosomes**

110 The SPI- and NI-loaded cubosomes were prepared using a high-pressure homogenization  
111 technique according to a slightly modified version of a previously published method.<sup>21)</sup>  
112 Briefly, 900 mg of monoolein, 40 mg of SPI/NI and 100 mg of pluronic F-127 were added to  
113 a beaker containing 20 mL of chloroform, and the resulting mixture was manually agitated to  
114 give a solution. All of the processes to prepare NI-loaded cubosomes were conducted in

115 amber glass containers because NI has high light sensitivity. The solvent was removed under  
116 reduced pressure on a rotary evaporator at 40–50 °C, and the resulting residue was dried  
117 under vacuum for 24 h at 20 °C to allow for complete removal of the organic solvent. The  
118 dried sample was dispersed in 200 mL of Milli-Q hot water with 80 °C, and premixed at 6000  
119 rpm for 6 min using a Speed Stabilizer (Kinematica<sup>®</sup> Co., Luzern, Switzerland). The coarse  
120 dispersions were also passed through a high-pressure homogenizer (Microfluidizer<sup>®</sup>  
121 Microfluidics Corporation, Newton, MA, USA) at 35 MPa with eight pass cycles. Finally, the  
122 cubosome materials were filtered through a 0.45- $\mu$ m membrane filter unit and stored in the  
123 dark at 20 °C prior to use.

#### 124 **Particle Size Distribution and Zeta Potential Measurements**

125 The mean particle size, PDI and zeta potential values of the different cubosomes were  
126 measured by dynamic light scattering (DLS) using a Zetasizer Nano ZS90 (Malvern  
127 Instruments, Malvern, UK) at 25 °C. The cubosome samples were diluted with Milli-Q water  
128 by 100-fold and measurements were performed at 25 °C. Each experiment was performed in  
129 triplicate.

#### 130 **Small-angle X-ray Scattering Measurements**

131 Small-angle X-ray scattering (SAXS) analyses were conducted to characterize the liquid  
132 crystalline phases of the cubosomes using a NANO-Viewer system (Rigaku, Tokyo, Japan)  
133 according to a previously reported method.<sup>7)</sup> Twenty microliter samples of the cubosomes  
134 were placed in a polyimide tube of 1 mm in diameter. The distance between the sample and  
135 the detector was set to 510 mm and the system was calibrated using powdered silver behenate.  
136 The temperature and exposure time were adjusted to 25 °C and 5 min, respectively. The  
137 lattice parameters of the cubic phase were calculated together with their standard error values  
138 using the Grafit 5 software (Erithacus<sup>®</sup> Software, Horley, Surrey, UK).

139

140 **Quantitative Evaluation of SPI and NI by HPLC**

141 SPI-loaded cubosome samples were diluted as necessary with acetonitrile and thoroughly  
142 mixed before being filtered through a 0.45- $\mu$ m membrane filter unit. The concentration of  
143 SPI in each sample was quantified by HPLC analysis using a TSKgel ODS-80Tm<sup>®</sup> column  
144 (4.6  $\times$  150 mm) on a Shimadzu LC-2010C HT<sup>®</sup> system (Shimadzu Corporation, Kyoto,  
145 Japan). The column was eluted with a mobile phase composed of a 7:3 (v/v) mixture of  
146 acetonitrile and water at a flow rate of 0.8 mL/min with an injection volume of 40  $\mu$ L. The  
147 column heater and UV-detector were set at 40 °C and 238 nm, respectively.

148 NI-loaded cubosome samples were diluted as necessary with methanol and thoroughly  
149 mixed before being filtered through a 0.45- $\mu$ m membrane filter unit. The concentration of NI  
150 in each sample was measured by HPLC analysis using a Cadenza CD-C18 column (3  $\times$  150  
151 mm) on a Shimadzu LC-2010C HT<sup>®</sup> system. The column was eluted with a mobile phase  
152 composed of a 3:2 (v/v) mixture of methanol and water containing 0.2% formic acid at a flow  
153 rate of 0.4 mL/min with an injection volume of 40  $\mu$ L. The column heater and UV-detector  
154 were set at 40 °C and 236 nm, respectively. All of the samples were quantified in triplicate.

155 **Quantitative Evaluation of SPI and NI by LC-MS/MS**

156 The SPI concentration was determined by LC-MS/MS using an API-3000 system (Agilent  
157 Technologies, Santa Clara, CA, USA) equipped with a Develosil ODS-HG-5 column (4.6  $\times$   
158 150 mm). The system was eluted with a mobile phase composed of a 3:2 (v/v) mixture of  
159 methanol and water containing 0.1% formic acid at a flow rate of 0.4 mL/min. The column  
160 temperature and run time were set to 28 °C and 15 min, respectively. The conditions for the  
161 LC-MS/MS were as follows: interface, turbo spray; ionization mode, ESI in the positive ion  
162 mode; ion source, nebulizer gas, curtain gas, collision gas; ionspray voltage, 5000 V;  
163 temperature, 350 °C; measurement mode, MRM method. The analytes were detected as  
164 follows: *m/z* values of 417.4 and 341.4 for the precursor ion and the product ion of SPI,

165 respectively. For *in vivo* pharmacokinetic study, we measured the concentration of canrenone  
166 (CAN), a major metabolite of SPI, using a slightly modified version of this method, where  
167 the column temperature, flow rate and sample run time were set to 35 °C, 0.5 mL/min and 25  
168 min, respectively. The analytes were detected as follows: *m/z* values of 341.3 and 107.1 for  
169 the precursor ion and the product ion of CAN, respectively.

170 The NI concentration was determined by LC-MS/MS analysis as above using a Cadenza  
171 CD-C18 column (3 × 150 mm) column. The system was eluted with a mobile phase  
172 composed of a 3:2 (v/v) mixture of methanol and water containing 0.1% formic acid at a flow  
173 rate of 0.4 mL/min. The column temperature and sample run time were set to 40 °C and 20  
174 min, respectively. The conditions for the LC-MS/MS were as follows: interface, turbo spray;  
175 ionization mode, ESI in the positive ion mode; ion source, nebulizer gas, curtain gas,  
176 collision gas; ion spray voltage, 5000 V; temperature, 300 °C; measurement mode, MRM  
177 method. The analytes were detected as follows: *m/z* values of 347.1 and 254.2 for the  
178 precursor ion and the product ion of NI, respectively. All of the quantification experiments  
179 were performed in triplicate.

### 180 **Drug Encapsulation Efficiency**

181 The cubosome preparations consisted of a mixture of encapsulated and free drug (un-  
182 encapsulated) fractions. The drug encapsulation efficiency (EE) of the cubosomes was  
183 determined based on the amounts of encapsulated and free drug by the ultra-centrifugation  
184 method. Briefly, a 4.0-mL sample of cubosome was placed in an Amicon Ultra-4 Centrifugal  
185 Filter-100K device (Merck Millipore Ltd, Carrigtwohill, Ireland) and centrifuged at 1057 ×*g*  
186 for 30 min using an Eppendorf centrifuge (Hamburg, Germany). The concentration of free  
187 drug present in the filtrate was determined by LC-MS/MS as described above. The  
188 percentage drug encapsulation efficiency of the cubosome was calculated using the following  
189 equation:



$$EE (\%) = \frac{D_{\text{total}} - D_{\text{free}}}{D_{\text{total}}} \times 100$$

190 where  $D_{\text{total}}$  is the total drug concentration of the sample before centrifugation and  $D_{\text{free}}$  is the  
191 free drug concentration in the filtrate after centrifugation. These experiments were conducted  
192 in triplicate.

### 193 **Stability Studies of the SPI- and NI-loaded Cubosomes**

194 The SPI- and NI-loaded cubosomes were stored at 20 °C in the dark prior to use and their  
195 mean particle size and PDI values were measured at 0, 1, 2, 3 and 4 weeks using the methods  
196 described above.

### 197 ***In Vitro* Release of SPI and NI from Cubosomes**

198 The *in vitro* release characteristics of the monoolein cubosome samples were examined  
199 using a membrane dialysis method with a variety of different release media, including 0.1 M  
200 sodium acetate buffer (pH 4.0), fasted state simulated intestinal fluid (FaSSIF) (pH 6.5) and  
201 fed state simulated intestinal fluid (FeSSIF) (pH 5.0) at 37 °C. The biorelevant FaSSIF and  
202 FeSSIF media were prepared in accordance with a previously reported protocol.<sup>22)</sup> Briefly, a  
203 1.0-mL sample of cubosome was added into a dialysis membrane bag (MWCO 14 kDa,  
204 Viskase Companies Inc., Darien, IL, USA), which was clamped at both ends before being  
205 submerged in 200 mL of release medium in a beaker. The beaker was then placed in a shaker  
206 bath at 37 °C and shaken horizontally at 100 strokes min<sup>-1</sup>. One-milliliter aliquots of release  
207 medium were withdrawn for analysis from each beaker at 1, 2, 4, 6, 12, 24, 48, 72 and 96 h,  
208 and replaced with the same volume of fresh medium. The collected samples were instantly  
209 diluted with acetonitrile for SPI or methanol for NI and filtered through a 0.45- $\mu\text{m}$  membrane  
210 filter. Finally, the concentration of drug released into the release medium was determined by  
211 HPLC as described above. These experiments were conducted in triplicate.

212

213

## 214 ***In Vivo* Pharmacokinetic Study**

215 Male Sprague-Dawley rats (weight: 280–310 g, age: 8–9 weeks; Japan SLC, Shizuoka,  
216 Japan) were fasted overnight for 12 h prior to the experiment. All of the procedures used in  
217 this study were performed in accordance with the guidelines approved by the Institutional  
218 Animal Care and Ethical Committee of the University of Shizuoka, Japan. SPI and NI  
219 dispersions were prepared at a concentration of 180  $\mu\text{g}/\text{mL}$  by dispersing these materials in  
220 Milli-Q water as controls for the SPI- and NI-loaded cubosomes. The SPI- and NI-loaded  
221 cubosome, as well as the corresponding controls, were orally administered to the rats at doses  
222 corresponding to 1 and 0.5 mg/kg of SPI and NI, respectively. Following the administration  
223 of these formulations, blood samples were collected *via* the tail vein at 1, 5, 10, 30, 60, 90,  
224 120, 180 and 240 min in Eppendorf tubes containing the anticoagulant heparin. The blood  
225 samples were then centrifuged at 4 °C and 4226  $\times g$  for 10 min to obtain plasma. The plasma  
226 samples were immediately treated with methanol and mixed by vortexing for 2 min, before  
227 being centrifuged at 4 °C and 4226  $\times g$  for 10 min. The supernatant was collected and filtered  
228 through a 0.20- $\mu\text{m}$  membrane filter unit. We determined the concentration of CAN and NI in  
229 the filtrate by LC-MS/MS using the method described above. The main pharmacokinetic  
230 parameters, including the maximum peak plasma concentration ( $C_{\text{max}}$ ), time of peak plasma  
231 concentration ( $T_{\text{max}}$ ), half-life ( $t_{1/2}$ ) and the area under the plasma concentration-time curve,  
232 were calculated using the linear trapezoidal rule from time zero to infinity ( $AUC_{0 \rightarrow \infty}$ ) and  
233 analyzed using the Win Nonlin<sup>®</sup> Pharmacokinetic program.

## 234 **Statistical Analysis**

235 Statistical analyses were performed using the Student's *t*-test. A probability value of  
236  $p < 0.05$  was considered to indicate statistical significance.

237

238

## 239 **Results and Discussion**

### 240 **Characterization of SPI- and NI-loaded Cubosomes**

241 The results for the characterization of the SPI- and NI-loaded cubosome particles are  
242 shown in Table 1. The mean particle size, PDI and zeta potential values of the SPI- and NI-  
243 loaded cubosomes were almost identical to those of the blank cubosomes. These data show  
244 that the encapsulation of drug molecules in the monoolein cubosomes had no impact on their  
245 mean particle size, PDI or zeta potential. It is noteworthy that the PDI values of SPI-loaded,  
246 NI-loaded and blank cubosomes were less than 0.3, indicating that they were monodispersed.

247 The SAXS patterns and lattice parameters of the SPI-loaded, NI-loaded and blank  
248 cubosomes are shown in Fig. 1 and Table 2, respectively. The SAXS patterns of all three  
249 materials showed three Bragg peaks with relative positions at spacing ratios of  $\sqrt{2}:\sqrt{4}:\sqrt{6}$ .  
250 These peaks were indexed according to the Miller indices  $(hkl) = (110), (200)$  and  $(211)$   
251 reflections, which were indicative of the body-centered cubic phase of the  $Im\bar{3}m$  space  
252 group.<sup>21)</sup> The encapsulation of SPI and NI molecules in the cubosomes had no discernible  
253 impact on their cubic space group. The lattice parameters of the cubic phase of the SPI-  
254 loaded cubosomes were slightly less than those of the blank cubosomes, whereas those of the  
255 NI-loaded cubosomes remained largely unchanged.

256 The apparent solubilities of SPI and NI increased when they were encapsulated in the  
257 monoolein cubosomes, as shown in Table 1. The encapsulation of SPI in the monoolein  
258 cubosomes led to a 6-fold increase in its solubility ( $28 \mu\text{g/mL}$  in water at  $25 \text{ }^\circ\text{C}$ ).<sup>23)</sup>  
259 Furthermore, the solubility of NI increased around 9-fold ( $20 \mu\text{g/mL}$  in water at  $25 \text{ }^\circ\text{C}$ )  
260 following its encapsulation in the monoolein cubosomes.<sup>24)</sup> The observed increases in the  
261 solubilities of these drugs could be attributed to the hydrophobic region of the cubic phase of  
262 monoolein. From a structural perspective, monoolein consists of a long hydrophobic aliphatic  
263 chain and a hydrophilic glycerol moiety. In the monoolein cubosomes, the hydrophobic

264 aliphatic chains would form a lipid bilayer with a cubic phase, with the hydrophilic glycerol  
265 moieties forming a water channel. Poorly water-soluble drugs such as SPI and NI would  
266 therefore be most likely incorporated into the hydrophobic lipid bilayer of the cubic phase of  
267 cubosomes, leading to an increase in the drug content of the hydrophobic lipid bilayer. The  
268 encapsulation efficiencies of the SPI- and NI-loaded cubosomes were 90.2 and 93.0%,  
269 respectively, highlighting the high solubility of these drugs in the lipid phase, as well as  
270 demonstrating that most of the drug molecules were encapsulated by the cubosome. The high  
271 encapsulation efficiencies of these cubosomes could be attributed to SPI and NI being highly  
272 lipophilic.

### 273 **Stability Study**

274 The mean particle size and PDI values of the SPI- and NI-loaded cubosomes remained  
275 largely unchanged for up to 4 weeks at 20 °C (Fig. 2). The results of the stability study  
276 indicated that the SPI- and NI-loaded cubosomes were more stable than the previously  
277 reported lipid nanoparticles. For example, the mean particle size of a suspension of NI-loaded  
278 lipid nanoparticles increased by around 14–30% after 30 days at 4 °C.<sup>25)</sup> Furthermore, the  
279 SPI-loaded liposomes were only stable at 5 °C.<sup>26)</sup>

### 280 ***In Vitro* Release of SPI and NI from Cubosomes**

281 The *in vitro* release profiles of SPI and NI are shown in Fig. 3. This result therefore  
282 demonstrates that NI was released at a greater rate into FaSSIF compared with the acetate  
283 buffer and FeSSIF. Although there appeared to be a decrease in the percentage of NI released  
284 from the cubosomes after 24 h, this phenomenon was attributed to the degradation of some of  
285 the NI released into the medium through hydrolysis or photolysis following the long  
286 incubation time. Moreover, the release profiles of the SPI- and NI-loaded cubosomes showed  
287 that no more than 5% of this drug was released into any of these media over 24 h, indicating  
288 that most of the drug particles remained encapsulated within the cubic phases of the lipid

289 bilayers of the monoolein cubosomes. This result also suggested that the cubosomes  
290 enhanced the solubility of SPI and NI, as stated earlier. The results obtained using the dialysis  
291 method for the *in vitro* release of these drugs from the cubosomes confirmed the drug  
292 encapsulation efficiency results determined by the ultra-centrifugation method (>90%). It has  
293 been reported that only 1.3% of the SN-38 molecules encapsulated in liposomes were  
294 released into the PBS buffer over 30 h, with the value reaching only 1.9% after 120 h.<sup>27)</sup> In  
295 contrast, the results of a later study showed that around 7% of the SN-38 molecules  
296 encapsulated in lipid nanocapsules were released into the PBS buffer over 24 h.<sup>28)</sup> Baskaran  
297 et al. (2014) reported that only 2.04% of the curcumin molecules encapsulated in monoolein  
298 cubic liquid crystalline nanoparticles were released into phosphate buffer saline at pH 7.4,  
299 with the rest of the drug molecules remaining unchanged within the nanoparticles.<sup>13)</sup>

### 300 ***In Vivo* Pharmacokinetic Study**

301 The oral bioavailabilities of the SPI- and NI-loaded cubosomes were investigated in rats  
302 and the results were compared with those of the corresponding pure drug dispersions. The  
303 pharmacokinetic parameters of these materials are shown in Table 3. The concentration of  
304 CAN, a major metabolite of SPI and NI, was determined at different time intervals in all four  
305 of these systems, and the results were plotted against time (Fig. 4). These results therefore  
306 implied that the oral bioavailabilities of SPI and NI increased considerably following the  
307 encapsulation of these drugs in the cubosomes. The mean  $AUC_{0-240\text{min}}$  and  $AUC_{0-\infty}$  values of  
308 cubosome-encapsulated drugs increased significantly compared with the corresponding  
309 cubosome-free dispersions (Table 3). The oral administration of a solid dispersion of NI (1  
310 mg/kg equivalent of NI) to rats was previously reported to give an  $AUC_{0-\infty}$  value of 31,676 ng  
311 min/mL. In this study, the oral administration of the NI-loaded cubosomes (0.5 mg/kg  
312 equivalent of NI) gave an  $AUC_{0-\infty}$  value of 58,540 ng min/mL, indicating that the formulation  
313 of NI with monoolein cubosomes led to a 4-fold increase in the  $AUC_{0-\infty}$  compared with a

314 solid dispersion of NI.<sup>29)</sup> Furthermore, the half-lives of the SPI- and NI-loaded cubosomes  
315 increased around 1.5-fold compared with the corresponding cubosome-free dispersions.  
316 Based on these results, we speculated that several factors could be responsible for the  
317 observed increases in the absorption characteristics of these two drugs.

318 Several mechanisms, acting in isolation or in combination, can lead to an increase in the  
319 oral bioavailability of a drug molecule. In terms of the SPI- and NI-loaded cubosomes  
320 prepared in the current study, the observed increases in the oral bioavailability could be  
321 attributed to the small size of the cubosome nanoparticles, which would allow them to enter  
322 into the intravascular spaces and strongly adhere to the gastrointestinal membrane, leading to  
323 an increase in the absorption of the drug molecules. The high affinity of the lipid-like  
324 gastrointestinal membrane for these hydrophobic drug molecules could also explain the  
325 observed increase in the bioavailability of these compounds. In particular, lipid-like  
326 nanoparticles such as the monoolein cubosomes used in this study have mucoadhesive  
327 properties that would lead to an increase in their contact time with the gastrointestinal  
328 membrane. These properties would therefore lead to an increase in the gastrointestinal  
329 residence time of the monoolein cubosomes, resulting in an increase in their oral  
330 bioavailability.<sup>9, 12)</sup> The plasma drug profiles of SPI and NI indicated that they were  
331 immediately absorbed, which could be attributed to the adsorption of the monoolein  
332 cubosomes onto the intestinal membranes. Last, the presence of lipids in the gastrointestinal  
333 tract such as the monoolein cubosomes can stimulate the secretion of bile into the small  
334 intestine from the gall bladder. The cubosomes could then interact with the bile salts to form  
335 mixed micelles, which could be absorbed together with the drugs into systemic circulation.<sup>30)</sup>  
336 Furthermore, the SPI- and NI-loaded cubosomes could favor lymphatic transport from the  
337 small intestine in a similar manner to that reported for other lipid-based formulations such as  
338 liposomes.<sup>18–20)</sup>

339 Although only small amounts of SPI and NI were released (<5%) from the monoolein  
340 cubosomes into the different release medium *in vitro*, the absorption of these drugs increased  
341 considerably compared with pure dispersions of the same materials. This disparity between  
342 the *in vitro* release profiles and the *in vivo* drug absorption characteristics could be attributed  
343 to the differences between the *in vitro* and *in vivo* environments, the latter of which is much  
344 more complex than the former. Furthermore, it is possible that the cubic phase of the  
345 monoolein cubosomes could be converted to a different phase (e.g., hexagonal phase) by one  
346 of the many compounds found in the gastrointestinal tract.<sup>31)</sup> This would result in the rapid  
347 release of SPI and NI, leading to an increase in their bioavailability. Furthermore, the  
348 absorption of these materials would be regulated by gastric emptying and intestinal transit  
349 time, which could explain the differences observed in the *in vitro* release profiles and *in vivo*  
350 drug absorption characteristics of these materials.<sup>32)</sup> We also observed small deviations in the  
351 absorption peaks of SPI and NI at 30 and 180 min, respectively, which could be attributed to  
352 the complex nature of the *in vivo* environment. Although the mechanisms responsible for the  
353 observed increases in bioavailability of SPI and NI from the cubosomes remain unclear, it is  
354 envisaged, based on the results of this study, that these cubosomes could potentially be used  
355 as suitable carriers for improving the oral bioavailabilities of SPI and NI.

356

## 357 **Conclusion**

358 The results of this study show that monoolein cubosomes containing SPI and NI in the  
359 cubic phase of their lipid bilayer enhanced the solubility and oral bioavailability  
360 characteristics of both of these drugs. SAXS analyses confirmed that these cubosomes existed  
361 in the cubic  $Im\bar{3}m$  space group and that they retained their structure after the addition of the  
362 drugs. In terms of their physicochemical properties, the mean particle sizes of these  
363 cubosomes were less than 100 nm and their PDI values were less than 0.3, which indicated

364 that they were monodispersed. The cubosomes also had zeta potentials in the range of –10 to  
365 –16 mV. The *in vitro* release profiles of the SPI- and NI-loaded cubosomes showed that they  
366 lost less than 5% of their encapsulated drugs into a variety of different media over 12–48 h.  
367 *In vivo* pharmacokinetic results also suggested that these systems exhibited sustained plasma  
368 drug levels and enhanced oral bioavailability. The results of a stability study suggested that  
369 the particle size and PDI values of the SPI- and NI-loaded cubosomes remained stable for at  
370 least 4 weeks. The SPI- and NI-loaded cubosomes developed in this study therefore represent  
371 promising carrier systems for the efficient delivery of drugs for the treatment of hypertension  
372 and related diseases.

373

#### 374 **Acknowledgements**

375 We would like to thank the Ministry of Education, Culture, Sports, Science and  
376 Technology (MEXT) of Japan and the Uehara Memorial Foundation for providing doctoral  
377 scholarship and research fellowship to Md. Ashraf Ali, respectively. This research work was  
378 partly supported by the Japan Society for the Promotion of Science KAKENHI (Grant Nos.  
379 26460224, 26460039 and 26460226). We would like to express our gratitude to Dr. Naoto  
380 Oku, Professor and Head, Department of Medical Biochemistry, University of Shizuoka for  
381 the support of his laboratory in conducting dynamic light scattering (DLS) analysis.

382

#### 383 **Conflict of Interest**

384 The authors declare no conflict of interest.

385

#### 386 **References**

- 387 1. Mehnert W., Mäder K., *Adv. Drug Deliv. Rev.*, **64**, 83–101 (2012).
- 388 2. Leuner C., Dressman J., *Eur. J. Pharm. Biopharm.*, **50**, 47–60 (2000).



- 389 3. Khadka P., Ro J., Kim H., Kim I., Kim J. T., Kim H., Cho J. M., Yun G., Lee J., *Asian J.*  
390 *Pharm. Sci.*, **9**, 304–316 (2014).
- 391 4. Anton N., Benoit J. P., Saulnier P., *J. Control Release*, **128**, 185–199 (2008).
- 392 5. Melis Ç., Ali D. S., Seyda B., “Application of Nanotechnology in Drug Delivery,” Chap.  
393 1, ed. by Ali D. S., InTech, Rijeka, 2014, pp. 1–50.
- 394 6. Hartnett T. E., Ladewig K., O’Connor A. J., Hartley P. G., Mclean K.M., *RSC Advances*,  
395 **5**, 26543–26549 (2015).
- 396 7. Ali M. A., Noguchi S., Iwao Y., Oka T., Itai S., *Chem. Pharm. Bull.*, **64**, 577–584 (2016).
- 397 8. Luo Q., Lin T., Zhang C. Y., Zhu T., Wang L., Ji Z., Jia B., Ge T., Peng D., Chen W., *Int.*  
398 *J. Pharm.*, **493**, 30–39 (2015).
- 399 9. Karami Z., Hamidi M., *Drug Discovery Today*, **21**, 789–801 (2016).
- 400 10. Koynova R., Caffrey M., *Chem. Phys. Lipids*, **115**, 107–219 (2002).
- 401 11. Chong J. Y. T., Mulet X., Keddie D. J., Waddington L. J., Mudie S. T., Boyd B. J.,  
402 Drummond C. J., *Langmuir*, **31**, 2615–2629 (2015).
- 403 12. Nguyen T., Hanley T., Porter C. J. H., Larson I., Boyd B. J., *Journal of Pharmacy and*  
404 *Pharmacology*, **62**, 856–865 (2010).
- 405 13. Baskaran R., Madheswaran T., Sundaramoorthy P., Kim H. M., Yoo B. K., *Int. J.*  
406 *Nanomedicine*, **9**, 3119–3130 (2014).
- 407 14. Lai J., Lu Y., Yin Z., Hu F., Wu W., *Int. J. Nanomedicine*, **5**, 13–23 (2010).
- 408 15. Jin X., Zhang Z. H., Li S. L., Sun E., Tan X. B., Song J., Jia X. B., *Fitoterapia*, **84**, 64–  
409 71 (2013).
- 410 16. Lai J., Chen J., Lu Y., Sun J., Hu F., Yin Z., Wu W., *AAPS PharmSciTech*, **10**, 960–966  
411 (2009).
- 412 17. Yang Z., Chen M., Yang M., Chen J., Fang W., Xu P., *Int. J. Nanomedicine*, **9**, 327–336  
413 (2014).

- 414 18. Kim H., Kim Y., Lee J., *Asian J. Pharm. Sci.*, **8**, 96–103 (2013).
- 415 19. Porter C. J. H., Trevaskis N. L., Charman W. N., *Nature Rev. Drug Discovery*, **6**, 231–  
416 248 (2007).
- 417 20. Trevaskis N. L., Charman W. N., Porter C. J. H., *Adv. Drug Deliv. Rev.*, **60**, 702–716  
418 (2008).
- 419 21. Barauskas J., Johnsson M., Joabsson F., Tiberg F., *Langmuir*, **21**, 2569–2577 (2005).
- 420 22. Marques M., *Dissolution Technol.*, **11**, 16 (2004).
- 421 23. Limayem Blouza I., Charcosset C., Sfar S., Fessi H., *Int. J. Pharm.*, **325**, 124–131  
422 (2006).
- 423 24. Hecq J., Deleers M., Fanara D., Vranckx H., Amighi K., *Int. J. Pharm.*, **299**, 167–177  
424 (2005).
- 425 25. Funakoshi Y., Iwao Y., Noguchi S., Itai S., *Chem. Pharm. Bull.*, **63**, 731–736 (2015).
- 426 26. Laouini A., Jaafar-Maalej C., Sfar S., Charcosset C., Fessi H., *Int. J. Pharm.*, **415**, 53–61  
427 (2011).
- 428 27. Zhang J. A., Xuan T., Parmar M., Ma L., Ugwu S., Ali S., Ahmad I., *Int. J. Pharm.*, **270**,  
429 93–107 (2004).
- 430 28. Roger E., Lagarce F., Benoit J. P., *Eur. J. Pharm. Biopharm.*, **79**, 181–188 (2011).
- 431 29. Law S. L., Lo W. Y., Lin F. M., Chaing C. H., *Int. J. Pharm.*, **84**, 161–166 (1992).
- 432 30. Das S., Chaudhury A., *AAPS PharmSciTech*, **12**, 62–76 (2011).
- 433 31. Chen Y., Ma P., Gui S., *Biomed Res. Int.*, **2014**, article ID 815981, 12 pages, (2014).
- 434 32. Cao X., Deng W. W., Fu M., Wang L., Tong S. S., Wei Y. W., Xu Y., Su W. Y., Xu X.  
435 M., Yu J. N., *Int. J. Nanomedicine*, **7**, 753–762 (2012).
- 436
- 437
- 438

439 **Figure Legends**

440 **Fig. 1. Intensity vs. the norm of the scattering vector obtained by SAXS measurements**  
441 **for the SPI-loaded, NI-loaded and blank cubosomes (without model drug).  $q=2 \sin\theta/\lambda$ ,**  
442 **where  $\theta$  is the Bragg angle and  $\lambda$  is the wavelength of X-ray.**

443

444 **Fig. 2. Changes in the mean particle size (line) and PDI (bar) values of the SPI-loaded**  
445 **cubosome (a) and the NI-loaded cubosome (b) up to 4 weeks at 20 °C. These data**  
446 **represent the mean values  $\pm$  S.D. ( $n=3$ ).**

447

448 **Fig. 3. *In vitro* release profiles of SPI (a) and NI (b) from the monoolein cubosomes in**  
449 **acetate buffer, FaSSIF and FeSSIF over 96 h at 37 °C. These data represent the mean**  
450 **values  $\pm$  S.D. ( $n=3$ ).**

451

452 **Fig. 4. *In vivo* drug release, a) plasma CAN concentration-time plot after an oral dose of**  
453 **1.0 mg/kg of the SPI-loaded cubosome and an SPI dispersion, b) plasma NI**  
454 **concentration-time plot after an oral dose of 0.5 mg/kg of the NI-loaded cubosome and**  
455 **an NI dispersion. These data represent the mean values  $\pm$  S.D. ( $n=5$ ).**

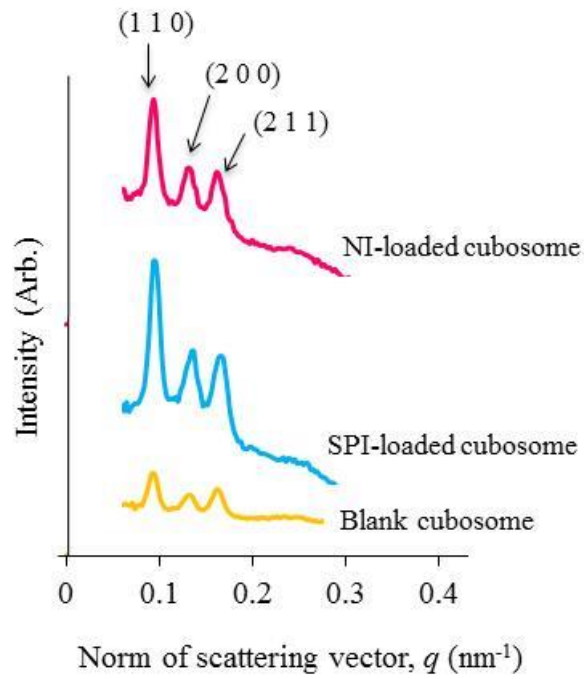


Fig. 1. Intensity vs. the norm of the scattering vector obtained by SAXS measurements for the SPI-loaded, NI-loaded and blank cubosome (without model drug).  $q=2 \sin\theta/\lambda$ , where  $\theta$  is the Bragg angle,  $\lambda$  is the wavelength of X-ray.

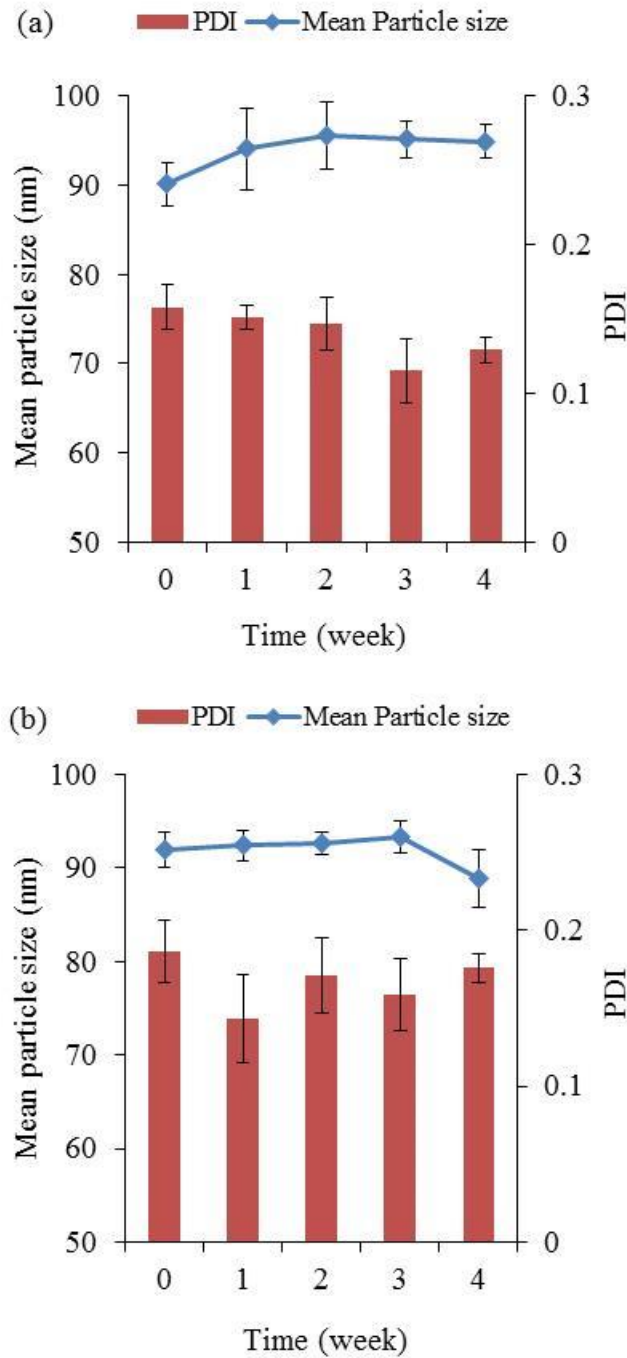


Fig. 2. Changes in the mean particle size (line) and PDI (bar) values of the SPI-loaded cubosome (a) and the NI-loaded cubosome (b) up to 4 weeks at 20 °C. These data represents the mean values  $\pm$  S.D. ( $n=3$ ).

457  
458  
459

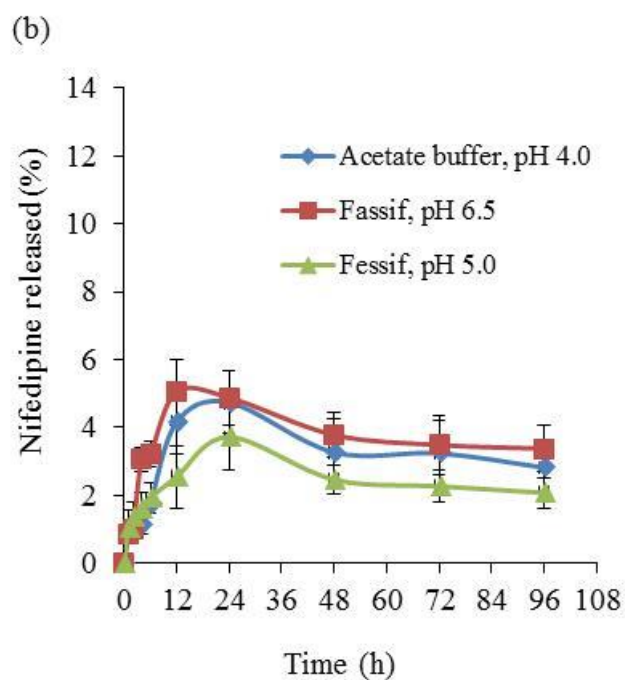
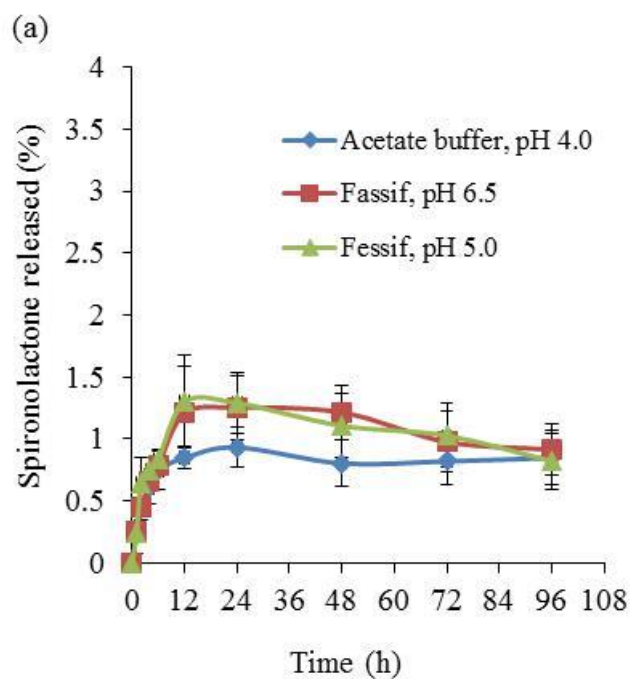


Fig. 3. *In vitro* release profiles of SPI (a) and NI (b) from the monoolein cubosomes in acetate buffer, FaSSIF and FeSSIF over 96 h at 37 °C. These data represents the mean values  $\pm$  S.D. ( $n=3$ ).

460  
461

462

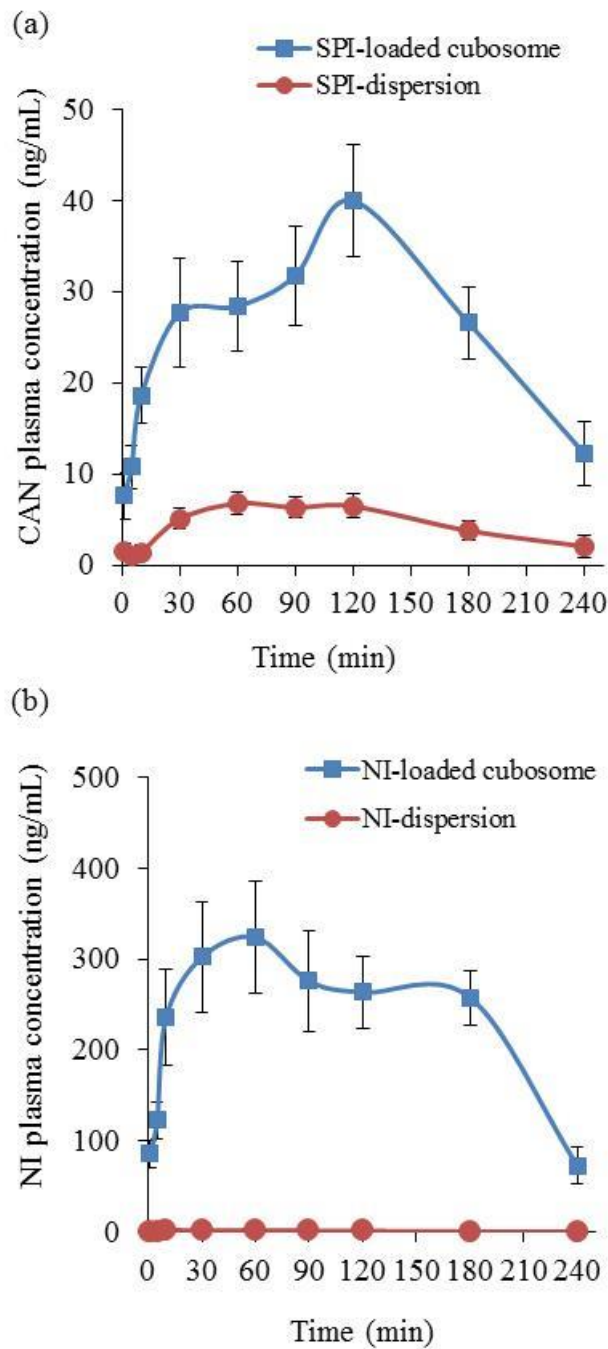


Fig. 4. *In vivo* drug release, a) plasma CAN concentration-time plot after an oral dose of 1.0 mg/kg of the SPI-loaded cubosome and an SPI dispersion. b) plasma NI concentration-time plot after an oral dose of 0.5 mg/kg of the NI-loaded cubosome and an NI dispersion. These data represents the mean values  $\pm$  S.D. ( $n=5$ ).